MC4TMD: Effects of Pythia8 generator configuration on reconstructed Transverse-Momentum-Dependent Parton Density Fuctions (TMD PDFs)

DESY Summer Student Programme, 2021

Sel Y.C. Zhou

University of Cambridge

Supervised by:

H. Jung

S. Taheri. Monfared

September 13, 2021

Abstract

In this study, PS2TMD method is validated by reconstructing TMDs from CASCADE3 parton showers (PS) and comparing to parton branching (PB) TMDs. Configuration dependence of TMD k_T distributions on Multi-Parton Interactions (MPI), primordial k_T, rapidity ordering, α_s order, and timelike showering are studied based on PYTHIA8 parton showers. Effects of intrinsic k_T width q_0 and color-ness of outgoing beam (Z boson vs. gluino) are also investigated with PYTHIA8. It is shown that MPI, primordial k_T, and timelike showering do not affect k_T distribution obtained as expected. Turning off rapidity ordering leads to a rise at the tail of distribution due to the inclusion of events that violate rapidity ordering. Next-to-Leading-Order (NLO) α_s distribution agrees with Leading-Order (LO) α_s distribution, while the 0^{th} order (fixed) α_s distribution exhibits different behaviors at different energy scale. TMDs for q_0=0.1 GeV and q_0=0.00001 GeV cases are consistent with each other while deviating from the default q_0=0.5 GeV case, which is slightly at odds with expectation. Z boson and gluino TMDs show similar configuration dependence and closely agreed results, indicating no color-ness discrimination in the toy model being used.

Contents

1 Introduction

1.1 Parton Density Functions and Parton Shower

The concept of 'parton' and its density functions earn their significance under the motivation to resolve internal structure of hadrons. The word 'parton' collectively refers to quarks and gluons - colored fundamental particles that can interact via QCD (quantum chromodynamics). As high energy physics evolves and accelerator technology boosts, it is hinted that hadrons - baryons and mesons - are not naively constituted of several valence quarks sticking together; they are rather messy assemblages of valence quarks, sea quarks and gluons. Therefore, the internal kinematics can no longer be a discrete sum over the valence quarks - a new formalism is needed to address this rising complexity, hence the proposal of parton theories.

Parton Density Functions (PDFs) are probability density functions for kinematic variables, i.e. energy fraction (x), transverse wave vector (k_T). The conventional form of PDF for a specific parton flavor, termed as 'co-linear PDFs', is written as $f_i(x, \mu^2)$, where i is the parton flavor, x the energy fraction (equivalently momentum fraction), and μ the virtuality. This functional form gives the probability to find the parton within x to x+dx and μ^2 to $\mu^2 + d\mu^2$. It reveals structural information for a hadron, encoding what it consists of and how its constituents are involved in internal dynamics. Different hadron models correspond to different PDF shapes, illustrated in Figure 1:

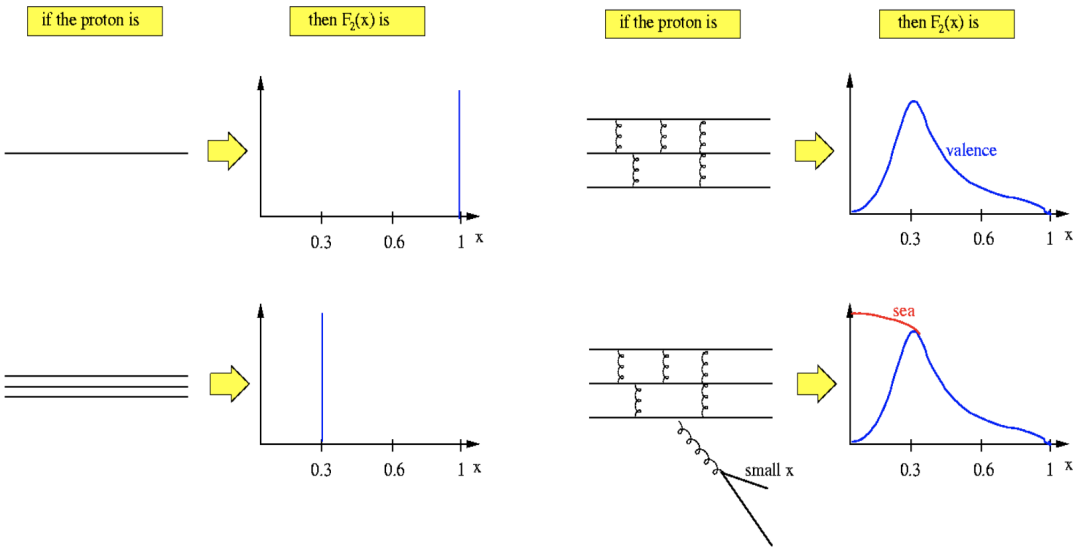

Figure 1: Comparison of different proton models and their corresponding PDF F_2 in x at a fixed μ^2 value. Reprinted from [5].

In the example of proton, we see that if the proton is a fundamental particle, it carries all the momentum itself, giving a delta spike at x=1 . If it is a simple combination of 3 valence quarks, each quark shall carry exactly one-third of the momentum, exhibiting a delta spike at x=0.33 .

On the right we see the PDfs when internal structures become complicated. If the three valence quarks are connected by gluons, the distribution still peaks at x=0.33 while smearing out to both sides. As sea quarks get involved, they cause the head of distribution to rise instead of going down on the left of x=0.33 .

PDFs are usually obtained from cross section factorisation in hard scatterings. In specific words, one solves DGLAP evolution equation and apply Next to Leading Order (NLO) / Next to Next Leading Order (NNLO) splitting functions. [6] This method applies to general PDFs - not only the co-linear PDF $f_i(x, \mu^2)$, but also Transverse-Momentum-Dependent (TMD) PDF $A_i(x, \mu^2, k_T)$ since it obeys a general evolution equation. Detailed discussion of TMD PDFS will be given in next section.

PDFs play an essential role to precisely describe hadronic collisions, typically involved in the formulation of **Deep-Inelastic-Scattering** (DIS, ep collision) and **Drell-Yan processes** (DY, pp collision), illustrated in Figure 2:

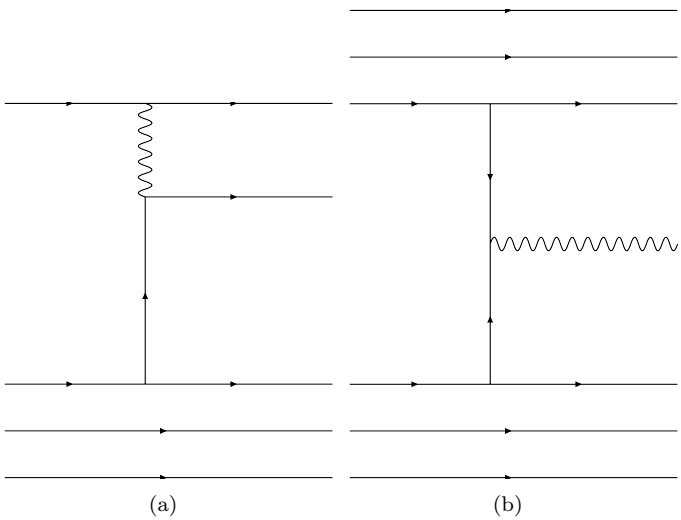

Figure 2: Feynman diagrams for (a) DIS: ep collisions and (b) Drell-Yan processes: pp collisions.

The diagrams depict the 'cleanest' scenarios. In reality, the parton is subjected to many secondary emissions along the way to hard scatterings. The most well-known ones are electromagnetic showers. Just like electric-charged particles capable of electromagnetic emissions, color-charged partons can emit QCD emissions, in the form of secondary partons. This type of emission gives rise to **parton shower** (PS) that is analogous to electromagnetic shower. A simple illustration is given in Figure 3. The formalism for PS will be elaborated in the section for **Parton Branching** (PB) method.

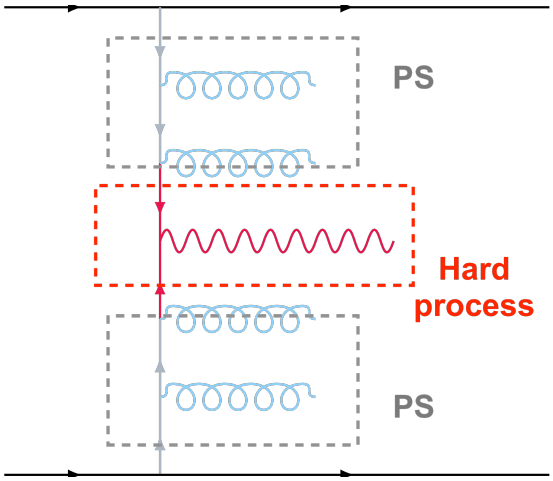

Figure 3: Illustration of PS. Only the two partons participating DY process are shown.

1.2 Transverse-Momentum-Dependent PDFs

Although co-linear PDFs work well when the beams are highly axial, its failure is spotted in certain physical scenarios. Two most representative examples are: **prediction of W/Z boson k_T spectrum** and **small x physics**. [2] They lead to the proposal of Transverse-Momentum-Dependent PDFs (TMD PDFs, or TMDs), which adds a new dependent variable k_T, transverse wavevector. It is written as $A_i(x, \mu^2, k_T)$, similar to co-linear PDFs.

W/Z boson k_T spectrum The k_T spectrum of W/Z boson can be divided into high k_T region, intermediate k_T region and low k_T region, illustrated in Figure 4. The high k_T region can be well described by finite order QCD perturbations combined with cross section factorisation using co-linear PDFs. Extending to intermediate k_T region where the spectrum peaks and further to low k_T region, the calculation diverges as multi-parton emissions gaining dominance. They can not be perturbatively described by a truncated QCD series, but require resummation over arbitrary number of parton emissions. This can be done with TMDs, and it was not until the application of TMDs that the correct W/Z boson k_T spectrum can be correctly predicted. [2]

Small x physics When x is large and the interactions are strongly co-linear, transverse momentum can be safely neglected without affecting kinematics. This is no longer the case for small x since transverse momentum becomes comparable. It is found that at small x, perturbative method gives rather large uncertainties due to the dominance of unordered multi-gluon emissions. To reconcile this, one must perform resummation with TMDs. [2]

Apart from the two examples, TMDs have wide application in many physical processes investigated at LHC, for instance, Higgs production and precise measurement of gluon fusions. It might also be extended to high k_T physics too. With no doubt we have exemplified the importance of understanding TMDs, which serves as the motivation for this study out of theoretical

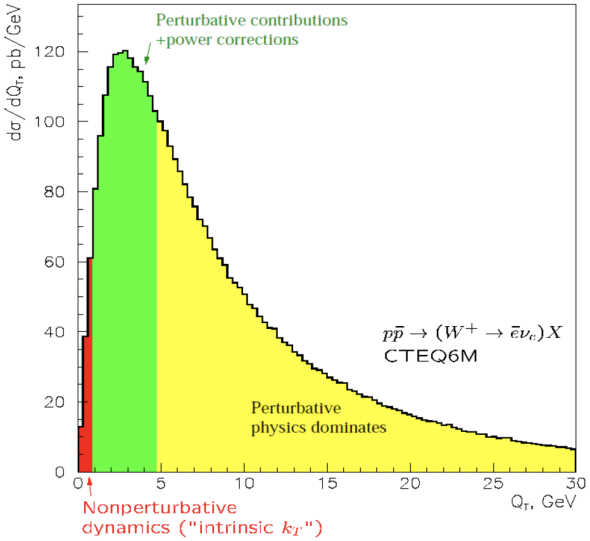

Figure 4: W boson k_T spectrum. Red: low k_T region, non-perturbative. Green: intermediate k_T region, perturbative + power corrections. Yellow: high k_T, perturbative. Reprinted from Fred Olness, CTEQ Summer School 2003.

interests. [2]

1.3 Monte-Carlo generator

A Monte-Carlo generator (MC generator) is a program that produces random events following a certain statistical distribution based on random number generators, statistics theories and physics rules. It turns theories into predictions of observables. The significance of MC generator is deeply enrooted in the foundation of modern physics and high-energy experimental methodology: It reflects the intrinsic, probabilistic nature of quantum theory which dominates the microscopic scale. It is also an integral part of experimental analysis in particle physics. In the case of particle physics, data comes from collider experiments, while theoretical predictions are given by MC generators, corrected by detector performance. The scrutiny between collider data and theoretical predictions draws a conclusion on the validity of current theories and existence of new physics.

Therefore, reliable theoretical predictions, or specifically, reliable MC generators are required. In the context of TMDs, MC generators are used to simulate PS and study TMD kinematics. From the phenomenologist's side, one must understand the MC generators well enough to distinguish between computational artifacts and real, physical processes in order to make sensible comparison with experimental results. This is the practical side of the motivation for this study.

The aim of this study is to showcase, with PYTHIA8, how event generator configuration affects the TMD distributions obtained. Different configurations are used to generate parton showers, then the TMDs are reconstructed from the parton shower using PS2TMD method and compared. This report is organized as such: Section 1 introduces the background and moti-

vation for this study; Section 2 explains the theories and methodology ; Section 3 elaborates on computational implementation of the methods ; Section 4 presents results for: 1) validation of methods, where PS2TMD is proved reliable, 2) Configuration Dependence Study, where different configurations are studied, 3) Model Dependence Study, where changes are made to the model process and their effects are observed; Section 5 and 6 discuss and conclude the results.

2 Methodology

2.1 Parton Branching

Parton Branching (PB) method provides a novel formulation of PDF evolution and PS. In simple words, PB and PS are merely evolving along opposite directions in energy scale μ, shown in Figure 5 in the context of pp collision.

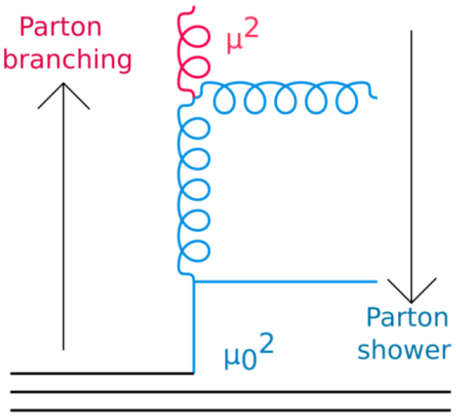

Figure 5: Cartoon showing the distinction between PB and PS. This diagram is essentially the lower part of Figure 3. One can clearly see that PB evolves from lower hadron scale μ_0^2 to hard process scale μ^2, while PS descends from μ^2 to μ_0^2. Reprinted from [8].

PB is forward evolution from hadron scale (low) to hard process scale (high), while PS is backward evolution. If the routine to compute PB is valid, one can reverse it to reliably reconstruct TMDs of proton constituents from the hard process data - in other words, to probe inside the proton using DY processes. While agreeing with conventional methods, PB method has additional features: At each branching, conservation of energy and momentum are enforced and the calculation of x and k_T are exact. It can also incorporate angular ordering that is suggested by color coherence.

In PB method, the DGLAP evolution equation can be iteratively solved to give

$$\begin{aligned}\mathcal{A}_a\left(x,\mathbf{k},\mu^2\right) = \Delta_a\left(\mu^2\right)\mathcal{A}_a\left(x,\mathbf{k},\mu_0^2\right) + \sum_b \int \frac{d^2\mathbf{q}'}{\pi\mathbf{q}'^2}\frac{\Delta_a\left(\mu^2\right)}{\Delta_a\left(\mathbf{q}'^2\right)}\Theta\left(\mu^2-\mathbf{q}'^2\right)\Theta\left(\mathbf{q}'^2-\mu_0^2\right) \\ \times\int_x^{z_M}\frac{dz}{z}P_{ab}^{(R)}\left(\alpha_s,z\right)\mathcal{A}_b\left(\frac{x}{z},\mathbf{k}+(1-z)\mathbf{q}',\mathbf{q}'^2\right)\end{aligned} \tag{1}$$

where $\mathcal{A}_a\left(x,\mathbf{k},\mu^2\right)$ is TMDs. $\Delta_a(\mu^2)$ is the Sudakov form factor that indicates the probability of no branching between μ_0 and μ, given by

$$\Delta_a\left(\mu^2\right) = \exp\left(-\sum_b\int_{\mu_0^2}^{\mu^2}\frac{d\mu'^2}{\mu'^2}\int_0^{z_M}dzzP_{ba}^{(R)}\left(\alpha_s,z\right)\right)$$

$\mathcal{A}_a\left(x, \mathbf{k}, \mu^2\right)$ is related to co-linear PDF through

$$f_a\left(x, \mu^2\right) = \int \mathcal{A}_a\left(x, \mathbf{k}, \mu^2\right) \frac{d^2\mathbf{k}}{\pi}$$

To obtain Monte-Carlo solution of Equation (1), initial parameters are required, yet it is too time-costly to test every possible set of initial parameters. Therefore, one first solves the kernel $\mathcal{K}_{ba}\left(x'', k_{t,0}^2, k_t^2, \mu_0^2, \mu^2\right)$ from the Monte-Carlo solution of initial parton with flavor b evolving into final parton with flavor a. Then one writes

$$\begin{aligned} x\mathcal{A}_a\left(x, k_t^2, \mu^2\right) &= x \int dx' \int dx'' \mathcal{A}_{0,b}\left(x', k_{t,0}^2, \mu_0^2\right) \mathcal{K}_{ba}\left(x'', k_{t,0}^2, k_t^2, \mu_0^2, \mu^2\right) \delta\left(x'x'' - x\right) \\ &= \int dx' \mathcal{A}_{0,b}\left(x', k_{t,0}^2, \mu_0^2\right) \frac{x}{x'} \mathcal{K}_{ba}\left(\frac{x}{x'}, k_{t,0}^2, k_t^2, \mu_0^2, \mu^2\right) \end{aligned}$$

where a Gaussian primordial k_T distribution is included via

$$\mathcal{A}_{0,b}\left(x, k_{t,0}^2, \mu_0^2\right) = f_{0,b}\left(x, \mu_0^2\right) \cdot \exp\left(-\left|k_{t,0}^2\right| / \sigma^2\right)$$

Here the Gaussian width is set as $\sigma^2 = q_0^2/2$ and $q_0 = 0.5$ GeV for all flavors. q_0 can be changed to other values, while the best fit is found to be at 0.5 GeV. [7] [6]

After calculating the MC solution, the unknown coefficients are obtained by fitting solution to HERA inclusive DIS measurements. [7]

The above method is applied to produce the two TMD sets used in this study, PB-NLO-HERAI+II-2018-set1 and PB-NLO-HERAI+II-2018-set2.

2.2 PS2TMD

PS2TMD method [8] is a routine proposed to extract effective TMDs from parton showers. It defines a toy process based on DY production of Z boson/gluino, shown in Figure 6:

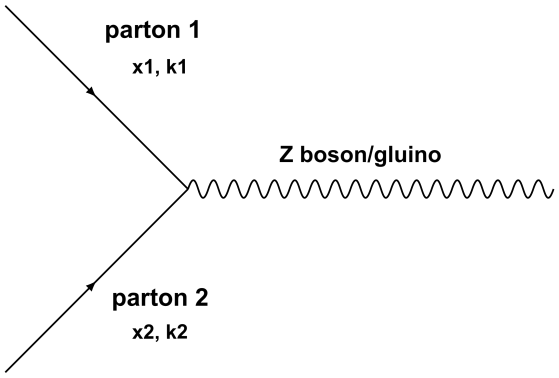

Figure 6: Feynman diagram of PS2TMD toy model.

The toy model describes a quark-antiquark pair annihilating to produce a Z boson or gluino when

parton showers are not included yet. Momentum conservation trivially gives

$$k_{2\perp} = k_{Z\perp} - k_{1\perp}$$

Knowing $k_{Z\perp}$ and $k_{1\perp}$ from MC generator event records, the $k_{2\perp}$ (in later sections simplified as k_T) can be calculated and histogrammed to obtain its TMD distribution. This is essentially how PS2TMD reconstructs TMDs from parton showers.

Now, switching on parton showers and fixing several parameters, the toy process is modified as Figure 7:

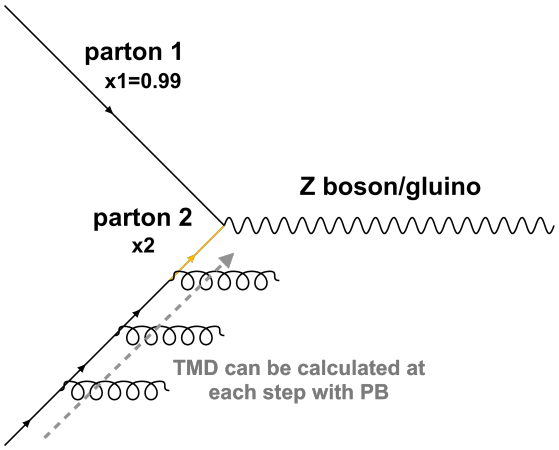

Figure 7: Feynman diagram of PS2TMD toy model when PS is included. The yellow parton is the one of which k_T distribution is studied. Curly lines attached to parton 2 represent parton emissions.

In this study, PS is only considered on parton 2 in the form of initial state radiation (ISR). x_1 is fixed to be 0.99. One asks the MC generator to produce process in Figure 7 according to PB TMDs, then apply momentum conservation condition to compute and reconstruct k_T distribution for the parton labelled yellow. To validate this method, one can compare the reconstructed distribution with the PB TMDs calculated step by step from PB evolution. They shall agree with each other. Details of the validation will be given in next section. In the configuration study, outgoing beam is set to be Z boson, and the gluino scenario is investigated in model dependence study.

2.3 Routine of this study

As mentioned, the purpose of this study is to illustrate how the configuration of MC generator affects the TMDs obtained from parton shower it generates. Hence, to understand the methodology, one must understand:

1. how parton shower is generated by MC generator
2. how TMDs are extracted from parton shower

They can be readily illustrated by Figure 8:

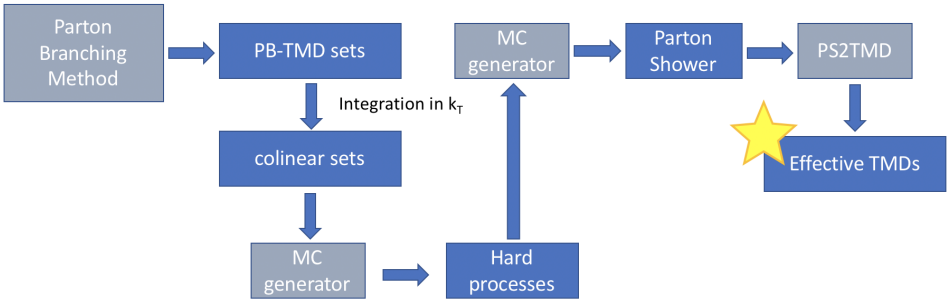

Figure 8: A flow chart for configuration studies, illustrating how parton showers are obtained from MC generator and how TMDs are constructed from the parton showers. The grey blocks represent a program/method while the blue blocks correspond to data/result.

For a study focused on a particular TMD set, the TMD set is first generated from PB method, then integrated over k_T to obtain a corresponding co-linear set, which is then fed into MC generator to produce hard process simulations. At this stage, the information of primordial k_T distribution is already lost in the integration. The simulated hard process data is correctly normalized corresponding to the initial TMD set, but it does not contain any information about primordial k_T distribution.

With the hard process data, MC generator produces parton showers by simulating ISR under given configurations, and the routine PS2TMD is applied to extract effective TMD from the parton showers. **The configuration dependence is studied by using different setups for the MC generator to produce parton showers, then comparing the different TMDs thereby obtained.**

Notice that the two MC generator blocks shown in Figure 8 are not necessarily the same generator. Different generators could be chosen to optimize the performance and suit specific interests.

Heretofore, an assumption has been made that PS2TMD routine is reliable, that it indeed produces the correct initial TMD from the parton shower. This assumption must be validated before conducting configuration studies. One can check the validity of PS2TMD by producing parton showers that exactly follow a specific TMD set, applying PS2TMD to reconstruct the TMD from parton showers, and comparing the reconstructed TMD with the one initially fed into the MC generator. The initial and reconstructed TMD sets are expected to be the same. This is illustrated in Figure 9:

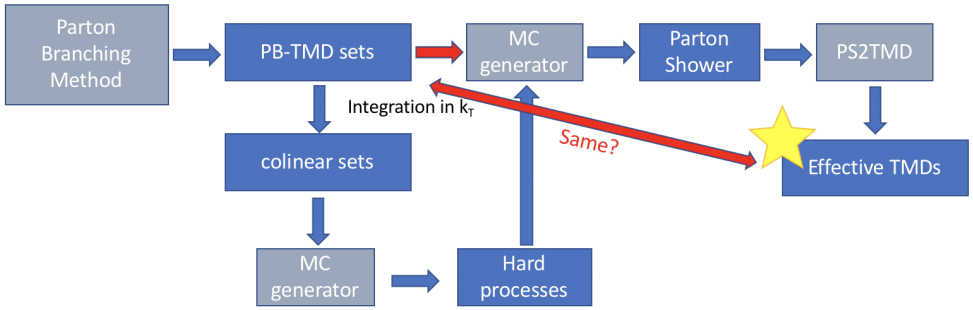

Figure 9: A flow chart illustrating the method for validation check.
The difference is marked by red arrows.

In Figure 9, one can clearly spot the difference that the original TMD set is also fed into the MC generator that generates parton shower, while it is not in the method of configuration studies. This generates parton showers that exactly follow a specific TMD set by enforcing kinematic limits accordingly in the production of parton showers.

In summary, the following investigations are conducted:

1. Validation check for PS2TMD with two different PB-TMD sets.
2. Configuration study for various setups with the same PB-TMD set.
3. Model dependence study by changing PB parameters and outgoing beam.

Model dependence study is performed to see if varying the toy model setups affects the TMD obtained from the same MC generator configuration. It serves as an interesting companion to the main study.

The configuration parameters to be investigated in the main study include:

- **Multi-Parton Interaction (MPI)** (Default: off)
- **Primodial** k_T (Default: on)
- α_s **order** (Default = 1, can be set to 0-2)
- **rapidity ordering** (Default: on)
- **timelike showering (FSR)** (Default: off)

They are selected since they are the most relevant 'switches' to the hard processes when generating parton showers, hence might affect TMDs. To study each configuration, it is changed from default value while keeping the rest unchanged, then TMDs are reconstructed and compared to

the ones produced by default parton showering (ISR on while others are kept default).

For model dependence study, initial k_T width q_0 is varied, and the final outgoing beam is also changed to gluino to see if a coloured final state changes TMDs.

3 Implementation

The idea of this study has been hitherto explained in general concepts. In this section, technical details will be covered to illustrate how exactly the simulations and analysis are accomplished.

The entire procedure of the main study, namely the investigation on configuration dependence, consists of three stages:

1. MC parton shower generation
2. TMD reconstruction
3. Reconstructed TMD plotting

The first two stages are based on DESY server while TMD plotting is performed with online TMD plotter (site address hyperlinked). [1] The first two stages produces a single data file, which is called a 'job'. To include enough statistics for stage 3, 2000 such jobs are done and all the data files obtained are merged for plotting. The details of implementation is visualized in Figure 10:

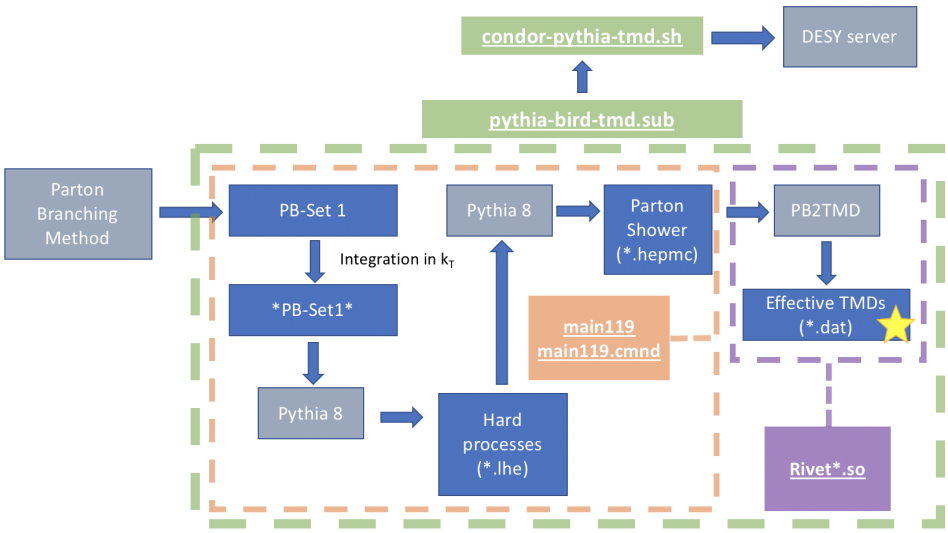

Figure 10: A flow chart illustrating the detailed technical implementation of the configuration dependence study. Previous blocks are substituted with the specific setups/programs being used. Data file extensions are shown in the brackets, and the underlined terms represent the functional scripts for processes inside each frame. Name of the scripts serves no technical purpose, therefore can be set arbitrarily.

As shown, the entire procedure for a single job is completed in one go, embodied in the script pythia-bird-tmd.sub. In this script, the processes are carried out through:

- **main119:** PYTHIA8 [9][10] executable - the program that runs PYTHIA8 - built from its

corresponding C++ script. The PB-TMD set fed into it can be changed to other TMD sets as well.

- **main119.cmnd:** command file that specifies the number of events to be generated and modifies configurations in main119. Number of events are set to 1000000 for all cases for statistical purpose. Different Pythia configurations of interests are obtained with this command file by coding relevant configuration changes inside it.
- **Rivet*.so:** Rivet3 [4] plugin that contains analysis routine (PS2TMD in this case), reconstructing TMDs. Since the TMD PDF function has 3 dependent variables, its value, along with x_2, μ, k_T, are stored in a 4-dimensional grid for plotting.

Subsequently, this pythia-bird-tmd.sub is passed to condor-pythia-tmd.sh, which is the file actually submitted to DESY server. This file specifies number of jobs, or equivalently number of .dat files, to be performed and merged for TMD plotter.

For validation check, the implementation is essentially the same except that the MC generator producing parton shower is CASCADE3 [3] instead of PYTHIA8. An extra steering file (command file) is included into the *.sub file to adjust the CASCADE3 settings. CASCADE3 is used here because PYTHIA8 cannot generate parton shower following a specific TMD distribution as required by this part of study.

This study is based on two PB-TMD sets, PB-NLO-HERAI+II-2018-set1 and PB-NLO-HERAI+II-2018-set2. They are both obtained from Parton Branching method and fitting to HERA Deep Inelastic Scattering data, bearing only the difference in the renormalization scale for α_s, which is evolution scale μ^2 for PB-set1 and transverse momentum k_T for PB-set2. [7] The two sets, together with their corresponding co-linear sets, are called PB-set1 and PB-set2. Both sets are used in validation check while the configuration dependence study and model dependence study concentrate on PB-set1.

For the investigation on model dependence, effect of q_0 values is examined by using different PB-TMD sets, at the very beginning, generated at different q_0 values with PB method, while the change to gluino is done in main119 executable for PYTHIA8.

4 Results

Since the effects of configurations are most noticeable in k_T distribution, plots for TMD PDF in k_T are given in this section to best showcase the results. Parton flavor is set to be gluon just for illustration purpose as we observe similar patterns for all parton flavors. All the plots are made with $k_T > 1$ GeV as the region below cannot be reliably reached by MC generators.

4.1 Validation check

As described, PYTHIA8 is used to produce the hard processes, and CASCADE3 is used for parton shower generation. Then TMDs are reconstructed with Rivet3. The results are given in Figure 11:

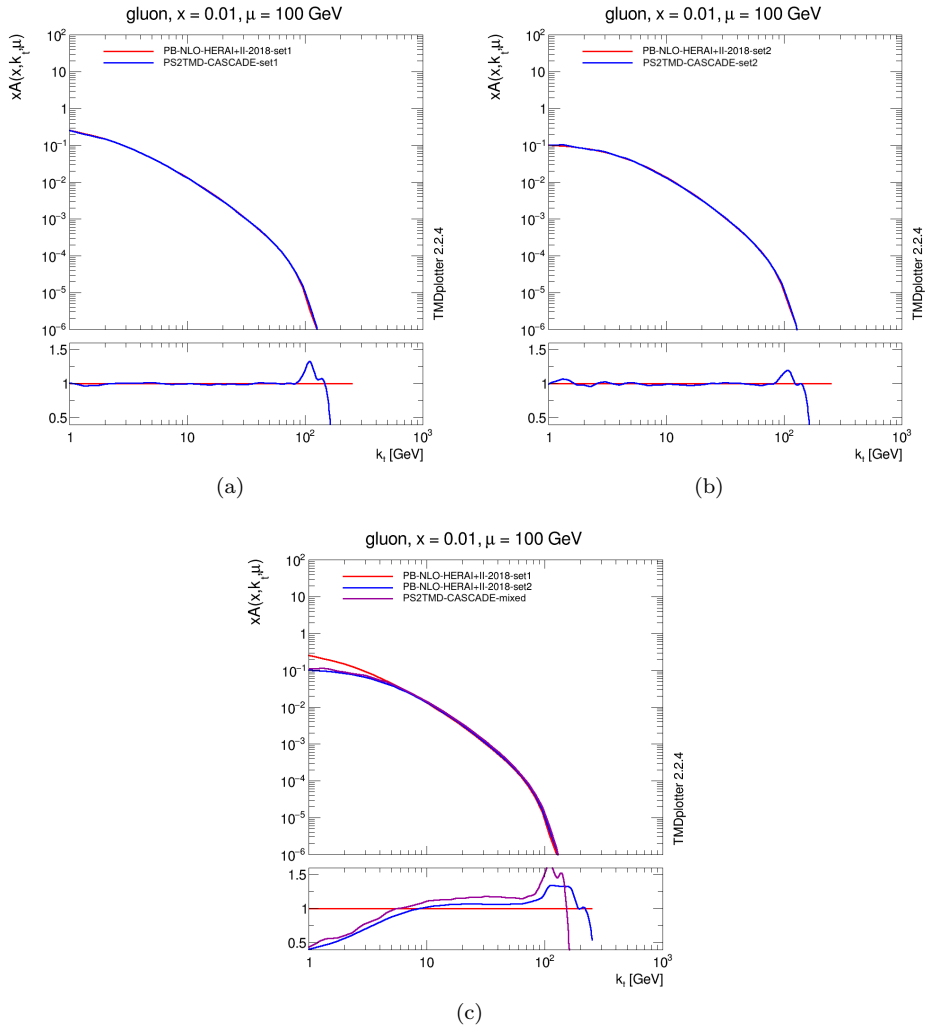

Figure 11: (a) PS2TMD validation result for PB-set1. (b) PS2TMD validation result for PB-set2. (c) PS2TMD result when the TMD sets are used inconsistently in the production of parton showers.

In Figure 11 (a), PB-set1 is used to generate hard processes and also fed directly into CASCADE3 to produce parton showers. This is done likewise in Figure 11 (b) with PB-set2. It is evident from those two figures that when TMD sets are used consistently, the reconstructed TMDs agree with the initial TMDs within less than 2% difference, validating PS2TMD method. In Figure 11 (c), PB-set1 is used for hard processes while PB-set2 is fed to CASCADE to generate parton shower. The reconstructed TMDs disagree with both of the PB-sets, as one would expect, since the calculation is itself inconsistent in physics.

For all plots in Figure 11 and the ones that follow up, fluctuations are seen at the tail. However, they do not imply inconsistency since the probability density has already fell to O(e-5), which is extremely sensitive to statistical uncertainties.

4.2 Configuration dependence

In this section, all results are generated with PB-set1 using PYTHIA8 as previously explained.

ISR default result In this part, the reconstructed k_T distribution from default parton showering is given in Figure 12. This is obtained by turning on ISR with the rest of the configurations set default.

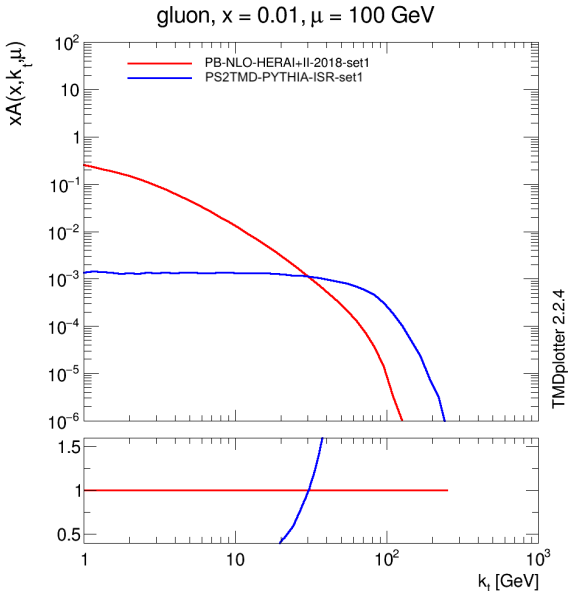

Figure 12: Reconstructed k_T distribution from default parton showering. Red line is PB-set1 and blue line is the reconstructed TMD from PYTHIA8.

In Figure 12, the original PB-set1 is considerably steeper than the effective TMD from PYTHIA8. One would expect to see this since they have adopted different ordering scheme - Parton Branching method is based on angular ordering while PYTHIA8 uses p_T ordering. Figure 12 indeed

illustrates the significance of ordering scheme in determining TMDs.

Since this study is based on PYTHIA8, p_T ordering is assumed, hence all the results shall be compared to the flatter PYTHIA8 effective TMD.

ISR + MPI ON result In this part, MPI is turned on for parton showering. Effective TMD is shown in Figure 13:

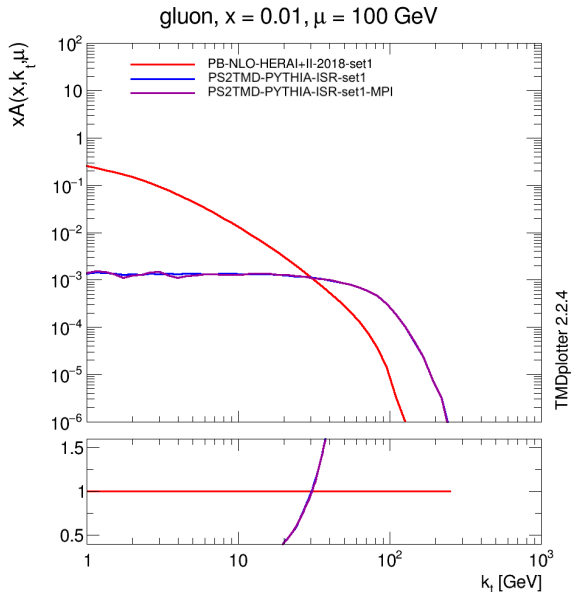

Figure 13: Reconstructed k_T distribution when Multi-Parton interactions are accounted.

One can see in Figure 12 that, despite small fluctuations below 10 GeV, MPI effective TMD closely agrees with the default parton showering, suggesting that it does not affect hard processes. This is indeed the case following definition of MPI, illustrated in Figure 14:

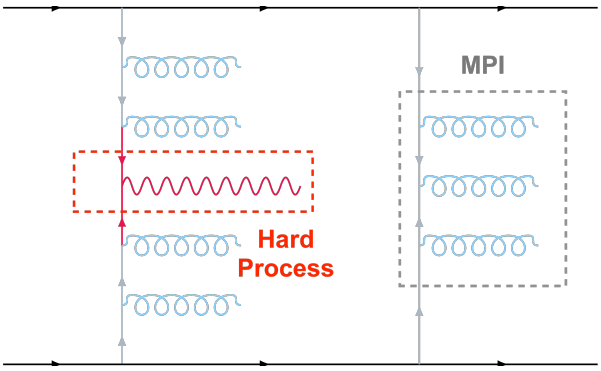

Figure 14: Cartoon illustrating MPI and hard process. Notice: this diagram is highly schematic.

It is straightforwardly shown that MPI does not affect hard processes, hence will not change the

TMDs.

ISR + Primordial k_T OFF result In this part, primordial k_T is turned off, that is, not assuming any particular distribution for parton 2's intrinsic k_T. Result is presented in Figure 15:

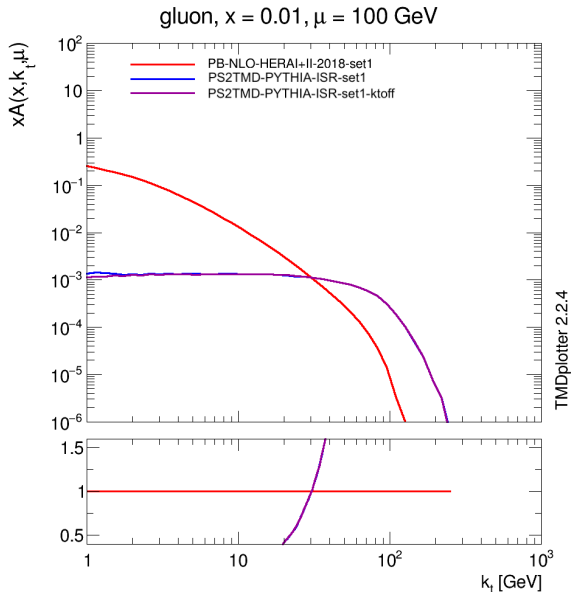

Figure 15: Reconstructed k_T distribution when primordial k_T is switched off.

Figure 15 suggests that primordial k_T does not affect the TMDs obtained. One would expect this conclusion as explained in Section 2, that the information of primordial k_T is already lost in the integration to co-linear set, hence tuning the this configuration shall not change hard processes by much.

ISR + α_s order result In this part, the order of strong coupling constant α_s is changed from default value. The value of this parameter indicates the order of α_s being used: 0 for 0^{th} order where α_s is fixed ; 1 (default value) for 1^{st} order/Leading Order (LO) where α_s takes the conventional value and changes with energy ; 2 for 2^{nd} order/Next-to-Leading Order (NLO) where 2^{nd} order loop expansion is included. The results for μ = 10, 100, 300, 800 GeV are given in Figure 16 to illustrate characteristic behaviors at different evolution scale. (See next page for the figure.)

From Figure 16, one see agreement between LO and NLO TMDs at all energy scales with small fluctuations below 10 GeV, which is not surprising since NLO is a further correction of LO, and the correction could be subtle when LO contribution dominates. The 0^{th} order α_s brings most significant impacts on the TMD obtained. In fact, the main difference between various evolution scales is how 0^{th} order α_s TMD differs from LO and NLO results:

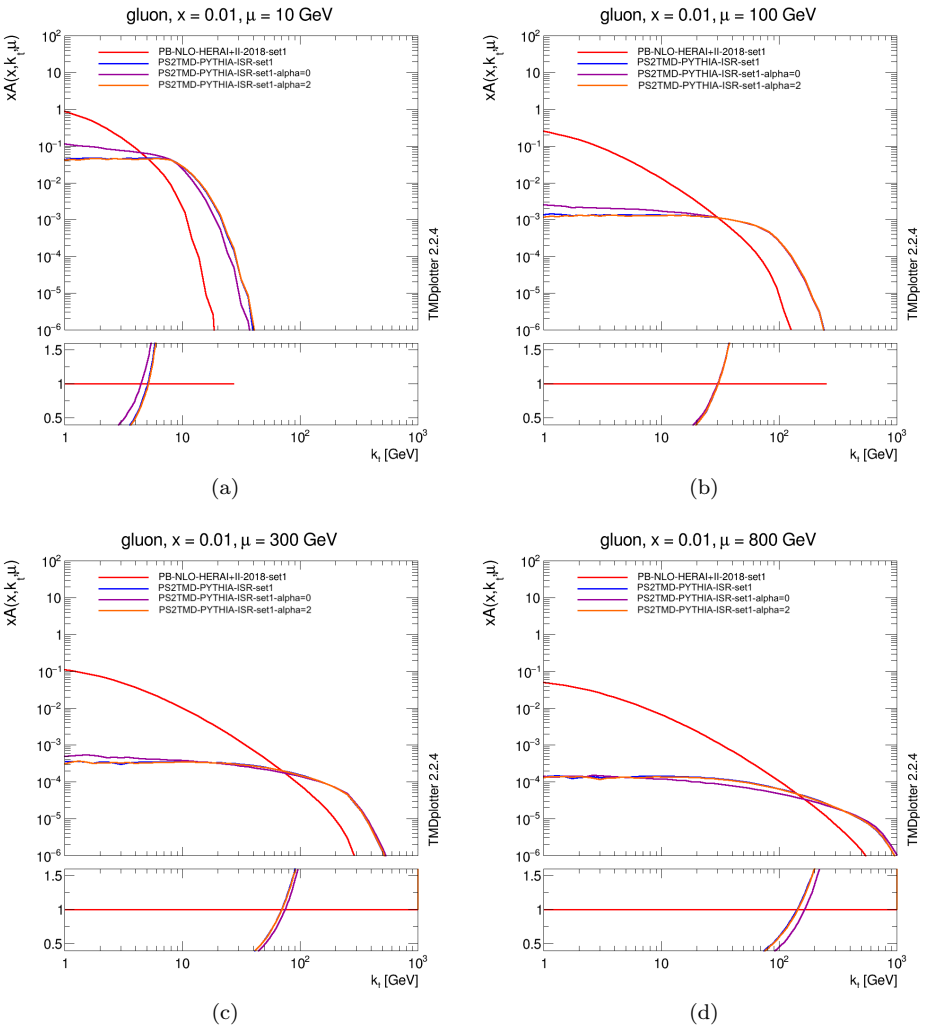

Figure 16: Reconstructed TMDs for different α_s orderings at (a) μ= 10 GeV, (b) μ= 100 GeV, (c) μ= 300 GeV, (d) μ= 800 GeV .

At low evolution scale $\mu \approx$ O(e1) to O(e2) GeV, the 0^{th}, 1^{st}, 2^{nd} α_s TMDs intersect at $k_{T,intersect} \approx \mu$, which is around 10 GeV in Figure 16 (a). Below $k_{T,intersect}$, 0^{th} probability density rises above the LO and NLO cases; Beyond $k_{T,intersect}$, 0^{th} probability density falls below.

At intermediate evolution scale $\mu \approx$ O(e2) to O(e3) GeV, an intercept $k_{T,intersect}$ is also seen between 10 GeV to 30 GeV. As μ increases, $k_{T,intersect}$ shifts toward left. Beyond $k_{T,intersect}$ the three TMDs converge, while below $k_{T,intersect}$ the 0^{th} order α_s result is still significantly higher.

At high evolution scale $\mu \approx$ O(e3) GeV, the three TMDs only agree at the two ends. In between, 0^{th} order α_s probability density is clearly lower than the other orders.

Therefore one can conclude that 0^{th} order α_s setting changes k_T distribution while 2^{nd} order does not at noticeable level.

ISR + rapidity ordering OFF result In this part, rapidity ordering is switched off and the results are given in Figure 17:

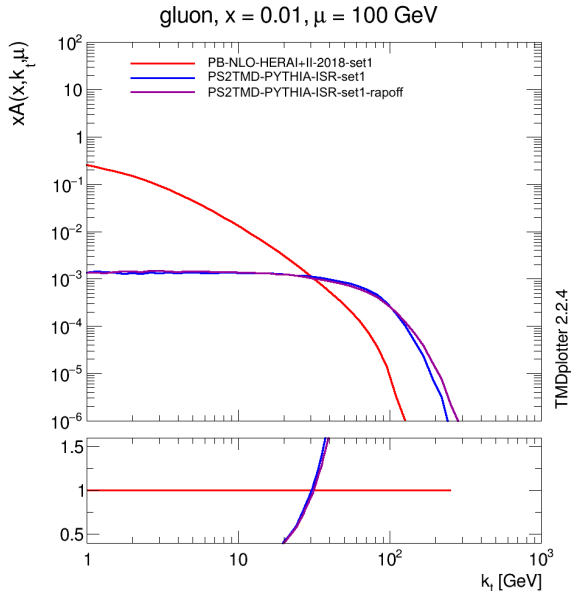

Figure 17: Reconstructed k_T distribution when rapidity ordering is switched off.

Figure 17 implies no difference between rapidity ordering ON and OFF below $k_T = \mu$. At the tail of distribution, turning off rapidity ordering leads to a higher probability density. This is attributed to the events that satisfy p_T ordering but not rapidity ordering, which are omitted when rapidity ordering is enforced. They are added back when rapidity ordering is OFF, hence giving a higher probability density.

ISR + FSR ON result In this part, timelike showering is turned on, and the result is shown in Figure 18. (See next page for the figure.)

Figure 18 shows good agreement between FSR TMD and default TMD with small fluctuations in low k_T region. It is acknowledged that the PYTHIA8 FSR configuration is ambiguous in whether the timelike showers are induced at initial state or final state. However, neither case affects hard processes, as illustrated in Figure 19.

It is therefore concluded that timelike shower does not affect TMD distribution obtained.

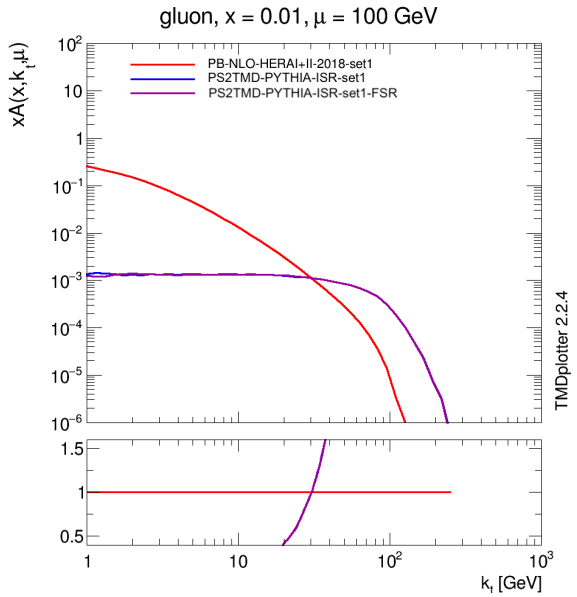

Figure 18: Reconstructed k_T distribution when timelike showering is switched on.

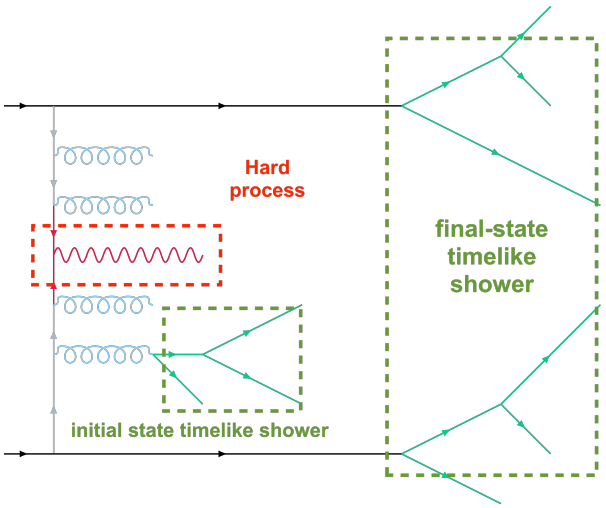

Figure 19: Illustration of hard process and timelike shower at initial state and final state. Notice: this diagram is highly schematic.

4.3 Model dependence

Effect of q_0 The Gaussian width of intrinsic k_T distribution, q_0, is varied to generated different initial PB-sets. Those PB-sets are identical to PB-set1 except for q_0 value. They are fed directly to CASCADE3 for PS generation. The co-linear set is produced from original PB-set1 since hard process does not concern k_T distribution, thus default PB-set1 would work just as fine. $q_0 = 0.1$, 0.00001 GeV PB-sets are investigated. The result is given in Figure 20:

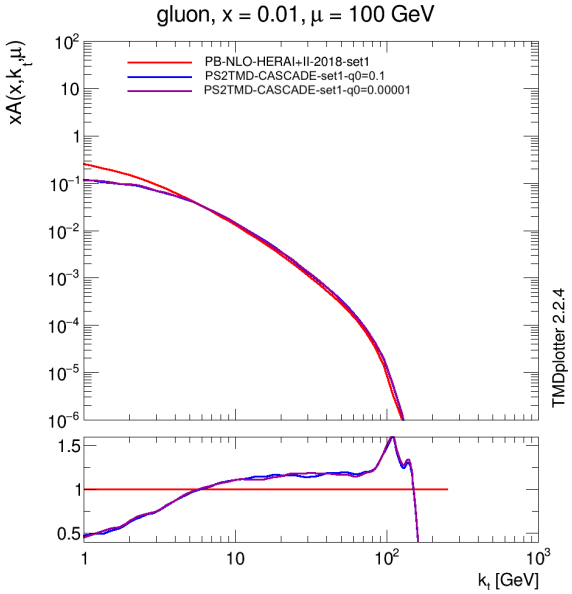

Figure 20: Effect of q_0 on k_T distribution.

One can patently see that TMDs for the two new q_0 values closely agree with each other but remarkably different from PB-set1, where $q_0 = 0.5$ GeV. This is peculiar at first glance since one might expect dramatic changes in k_T when q_0 is differed by several orders of magnitude. It is suspected a significant kinematic cut-off happens between $q_0 = 0.1$ and 0.5 GeV, hence below the cut-off certain processes are suppressed and q_0 value becomes irrelevant.

Gluino In the configuration study, the outgoing particle is Z boson. This could well be a colored object, such as supersymmetric particle gluino. Similar configuration study is therefore performed with outgoing gluino to see if color charges affect TMDs. The default ISR result, as well as accompanied configuration studies on **MPI, Primordial k_T, and rapidity ordering**, is given in Figure 21. (See next page for the plots.)

From the gluino plots one observes:

- Comparing between gluino TMDs with different configurations, one sees similar configuration dependence as in the Z boson case, that MPI and Primordial k_T do not change the distribution while turning OFF rapidity ordering leads to a rise at the tail.
- Comparing between gluino TMDs and Z boson TMDs with the same configuration adjust-

ment, one sees no discrepancy, which means the color-ness of outgoing particle is irrelevant in the construction of PS2TMD model.

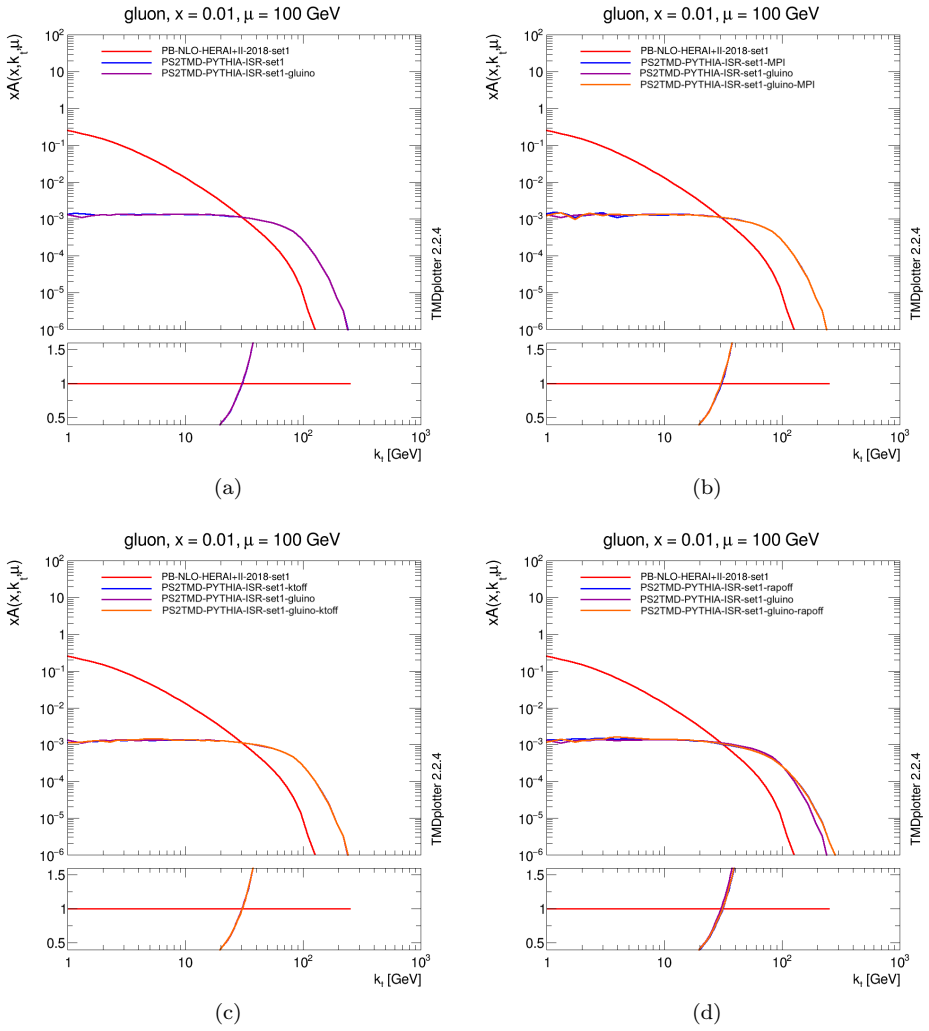

Figure 21: PS2TMD result for (a) default ISR parton showers (b) ISR + MPI parton showers (c) ISR + ktoff parton showers (d) ISR + rapoff parton showers. The blue line in all plots is the Z boson counterpart with the same configuration adjustment.

5 Discussion

Through the results, PS2TMD method has been validated as a routine to reliably reconstruct effective TMDs from parton showers, and PYTHIA8 behaves as expected for different configurations. Since this study goes no more beyond a preliminary investigation on PYTHIA8 performance, further examination in certain aspects is subject to discussion:

- An independent collaborator has performed a similar PYTHIA8 configuration study based on PB-set2. [11] When comparing the work, slightly greater fluctuations is always seen in the PB-set2, despite identical implementation, configuration setups, and volume of statistics. The source of fluctuation is unclear. It could be attributed to the difference in α_s renormalization scale when applying Parton Branching method, or other factors not considered in this work. Further investigation is required to pin down the cause of fluctuation.

- When comparing results with [8], it is noticed that the k_T distributions obtained in this study is significantly flattened out. While results from [8] plateau at O(e-2), the plateau in this study is at O(e-3), off by an order of magnitude. Hence, due to the unitarity of probability density function (which graphically manifests as conservation of area under curve), the tail of k_T distribution is comparatively 'pushed out'; the curve does not drop as fast as expected after reaching the evolution scale μ. The codes for two studies have been compared, yet the cause of this disagreement remains unclear. Notice that the results from independent collaborator are consistent with this study, showing similar disagreement with the previous study.

- Statistical uncertainty is not defined quantitatively in this study, hence the claims of consistency are 'loose' solely based on ratio (on the lower panel of plots). Further work should have uncertainty envelops embedded in Rivet plugin and quantitatively conclude consistency if two curves agree within the envelope.

- As mentioned in the model dependence study, it is not decisive why $q_0 = 0.1$ and 0.00001 GeV produce similar TMDs, potentially due to cut-offs of dominant kinematics, or other unconsidered factors. One shall further dive into the formalism of intrinsic distribution and relevant kinematics, and also repeat simulations with more q_0 values to locate the critical q_0 value that marks the change.

- The definition of timelike shower switch FSR, standing for Final State Radiation, is debatable - whether it treats timelike shower together including both initial state and final state timelike shower, or it only includes the final state timelike shower as the name of switch suggests. One shall examine PYTHIA8 documentation carefully to make clear of this point.

The rich content of this study has provided a sturdy playground for successors who are interested in QCD MC generators, with the reflections listed above serving as a good commence for continuing attempts.

6 Conclusion

With PYTHIA8 and CASCADE3 implementation, PS2TMD method is validated by reconstructing effective TMDs and comparing to the original PB-sets. The validation checks indicate PS2TMD can reliably extract TMDs from parton showers. Configuration dependence investigation is carried out with PYTHIA8 parton showers, concerning how MPI, Primordial k_T, α_s order, rapidity ordering, timelike showering affect the gluon k_T TMD PDF obtained. Results suggests that:

- MPI, Primordial k_T, timelike showering do not affect the k_T distribution obtained as they do not directly influence hard processes.
- LO and NLO α_s TMDs closely agree with each other, while the 0^{th} order α_s distribution exhibits different patterns as μ varies.
- Turning off rapidity ordering leads to a rise at the tail of distribution due to extra events allowed.

Model dependence study concludes that PS2TMD do not discriminate on color-ness of outgoing particle, based on almost identical TMDs obtained for Z boson and gluino, and similar configuration dependence seen on gluino TMDs. The effect of intrinsic k_T width q_0 is inconclusive. $q_0 =$ 0.1 GeV and 0.00001 GeV TMDs show noticeable deviation from the conventional $q_0 = 0.5$ GeV case, but no difference from each other.

Possible further efforts include: investigating the cause of PB-set2's larger fluctuation under identical setups, reconciling the disagreement with precious study [8], adding uncertainty envelops to quantitatively claim consistency, understanding the peculiar observation on q_0 values, and clarifying PYTHIA8's definition of FSR switch.

7 Acknowledgement

This report summarizes what is achieved in 2021 DESY summer school project B9 - MC4TMD. I would like to express my sincere thanks to the summer school committees, lecturers, and supervisors who have worked wholeheartedly to make everything possible under this harsh time of pandemics. I would also like to extend my deepest appreciation to my fantastic supervisors, Dr. Hannes Jung and Dr. Sara Taheri Monfared, who have provided us with tremendous amount of support, who have nurtured us as future physicists with tender words and kind hearts; and to my amazing collaborator Suzanne Steel, who always emanates inspiring energy and contagious passion along the path. Finally, I am extremely grateful to the entire B8 - B10 collaboration that is now voluntarily transformed into a global HEP student community. It is indeed shown that the very spirit of Science can be celebrated out of the most sincere and humble minds who, by nature persistently, seek for truth and love.

References

[1] N. A. Abdulov et al. *TMDlib2 and TMDplotter: a platform for 3D hadron structure studies.* 2021. arXiv: 2103.09741 [hep-ph].

[2] R. Angeles-Martinez et al. "Transverse Momentum Dependent (TMD) Parton Distribution Functions: Status and Prospects". In: *Acta Physica Polonica B* 46.12 (2015), p. 2501. ISSN: 1509-5770. DOI: 10.5506/aphyspolb.46.2501. URL: http://dx.doi.org/10.5506/APhysPolB.46.2501.

[3] S. Baranov et al. "CASCADE3 A Monte Carlo event generator based on TMDs". In: *The European Physical Journal C* 81.5 (May 2021). ISSN: 1434-6052. DOI: 10.1140/epjc/s10052-021-09203-8. URL: http://dx.doi.org/10.1140/epjc/s10052-021-09203-8.

[4] Christian Bierlich et al. "Robust Independent Validation of Experiment and Theory: Rivet version 3". In: *SciPost Physics* 8.2 (Feb. 2020). ISSN: 2542-4653. DOI: 10.21468/scipostphys.8.2.026. URL: http://dx.doi.org/10.21468/SciPostPhys.8.2.026.

[5] M. A. Douglas H.Francis. "Partons". In: *Quarks and leptons: An introductory course in modern particle physics.* John Wiley, 2016, p. 201.

[6] F. Hautmann et al. "Collinear and TMD quark and gluon densities from parton branching solution of QCD evolution equations". In: *Journal of High Energy Physics* 2018.1 (Jan. 2018). ISSN: 1029-8479. DOI: 10.1007/jhep01(2018)070. URL: http://dx.doi.org/10.1007/JHEP01(2018)070.

[7] A. Bermudez Martinez et al. "Collinear and TMD parton densities from fits to precision DIS measurements in the parton branching method". In: *Physical Review D* 99.7 (Apr. 2019). ISSN: 2470-0029. DOI: 10.1103/physrevd.99.074008. URL: http://dx.doi.org/10.1103/PhysRevD.99.074008.

[8] Melanie Schmitz. "Drell-Yan production with Transverse momentum Dependent Parton densities". PhD thesis. 2019.

[9] Torbjörn Sjöstrand, Stephen Mrenna, and Peter Skands. "PYTHIA 6.4 physics and manual". In: *Journal of High Energy Physics* 2006.05 (May 2006), pp. 026–026. ISSN: 1029-8479. DOI: 10.1088/1126-6708/2006/05/026. URL: http://dx.doi.org/10.1088/1126-6708/2006/05/026.

[10] Torbjörn Sjöstrand et al. "An introduction to PYTHIA 8.2". In: *Computer Physics Communications* 191 (June 2015), pp. 159–177. ISSN: 0010-4655. DOI: 10.1016/j.cpc.2015.01.024. URL: http://dx.doi.org/10.1016/j.cpc.2015.01.024.

[11] Suzanne Steel. *B9 MC4TMD: Determining Transverse Momentum Dependent Parton Distribution Functions (TMDs/ TMD PDFs) with Monte Carlo generators.* DESY summer school, 2021.